Proc. Natl. Acad. Sci. USA
Vol. 91, pp. 704–708, January 1994
Biophysics

Identification of histidine at the catalytic site of the photosynthetic oxygen-evolving complex

(histidine labeling/pulsed electron paramagnetic resonance/manganese/photosystem II)

XIAO-SONG TANG*, BRUCE A. DINER*, BARBARA S. LARSEN*, M. LANE GILCHRIST, JR.†, GARY A. LORIGAN†, AND R. DAVID BRITT†

*Central Research and Development Department, Experimental Station, P.O. Box 80173, E.I. DuPont de Nemours and Company, Wilmington, DE 19880; and †Department of Chemistry, University of California, Davis, CA 95616

Communicated by Pierre Joliot, October 26, 1993 (received for review September 13, 1993).

ABSTRACT **The molecular oxygen in our atmosphere is a product of a water-splitting reaction that occurs in the oxygen-evolving complex of photosystem II of oxygenic photosynthesis. The catalytic core of the oxygen-evolving complex is an ensemble of four manganese atoms arranged in a cluster of undetermined structure. The pulsed electron paramagnetic resonance (EPR) technique of electron spin-echo envelope modulation (ESEEM) can be used to measure nuclear spin transitions of nuclei magnetically coupled to paramagnetic metal centers of enzymes. We report the results of ESEEM experiments on the cyanobacterium *Synechocystis* PCC 6803 selectively labeled with ^{15}N at the two nitrogen sites of the imidazole side chain of histidine residues. The experiments demonstrate that histidine is bound to manganese in the oxygen-evolving complex.**

Photosynthetic oxygen evolution is a cyclic process involving five redox states, S_0 through S_4, where the subscript refers to the number of oxidizing equivalents that have accumulated on the oxygen-evolving complex (OEC) (1). These accumulate sequentially with each light-driven charge separation of the photosystem II (PSII) reaction center. Upon attaining the S_4 state an oxygen molecule is released, and the OEC returns to the S_0 state. The catalytic core of the OEC consists of a tetranuclear manganese cluster of undetermined structure. Electron paramagnetic resonance (EPR) signals arising from the manganese cluster of the OEC poised in the S_2 state have been observed in the $g = 2$ and $g = 4$ regions of the EPR spectrum (2–5). The first electron spin-echo envelope modulation (ESEEM) study of the $g = 2$ "multiline" signal, using PSII membranes isolated from spinach, revealed a broad structured peak centered near 5 MHz (6). This peak was shown to arise from ^{14}N by ESEEM experiments on PSII particles isolated from a thermophilic cyanobacterium (*Synechococcus* sp.) grown alternatively with $^{14}NO_3^-$ or $^{15}NO_3^-$ in the growth medium (7). The PSII particles prepared with natural abundance ^{14}N showed ESEEM spectra nearly identical with the ESEEM results from the PSII membranes of spinach. However, the 5-MHz modulation component was absent in the ESEEM patterns of the PSII particles globally enriched in ^{15}N. No new ^{15}N ESEEM peak replaced the 5 MHz ^{14}N peak. This is not surprising, because the moderate electric quadrupolar interaction of the spin $I = 1$ ^{14}N nucleus greatly enhances the state mixing needed to give rise to the spin-echo modulation (8–11). The hyperfine coupling needed to generate an ^{14}N spin transition at 5 MHz is comparable to the couplings observed with ESEEM to directly coordinated ^{14}N donor groups in synthetic Mn(III)Mn(IV) complexes (12, 13), indicating that the modulation most likely arises from a ligand to the manganese cluster rather than from a remote nitrogen site. Electron–nuclear double resonance (ENDOR) studies of a thermophilic cyanobacterium grown on $^{15}NO_3^-$ showed ^{15}N ENDOR transitions in the range 1–4 MHz (14). These ^{15}N ENDOR transitions most likely arise from the same nitrogen class or classes that give rise to the ^{14}N ESEEM peaks. Neither the ESEEM nor the ENDOR experiments provide a definitive chemical assignment to the origin of the nitrogen spin transitions. To assign the origin of these nitrogen spin transitions, we have incorporated into the PSII protein complex histidine in which both of the imidazole nitrogens were either ^{14}N- or ^{15}N-labeled.

MATERIALS AND METHODS

Isolation of a Histidine-Tolerant Strain. Labarre *et al.* (15) described the isolation of a histidine-tolerant mutant of *Synechocystis* PCC 6803 in which the transport of this normally toxic amino acid was impaired. As our application required incorporation of labeled histidine into cellular protein, we needed to both maintain histidine transport in a histidine-tolerant organism and suppress endogenous biosynthesis. The latter could be accomplished either through inactivation of genes involved in the biosynthetic pathway or through feedback inhibition of the pathway by the exogenous amino acid. A spontaneous histidine-tolerant strain showing feedback inhibition of the histidine biosynthetic pathway was obtained by growing wild-type cells photoautotrophically in BG-11 liquid culture medium (16) in the presence of 30 μM L-histidine. An aliquot of the cell suspension was plated on BG-11 agar Petri plates supplemented with 30 μM L-histidine, and a single colony was selected from those cells that grew. Further selection occurred by repeated transfers to plates containing increasing concentrations of L-histidine up to 240 μM.

Preparation of PSII Oxygen-Evolving Core Complexes. The histidine-tolerant strain was grown photoautotrophically in two 10-liter batches of BG-11 medium bubbled with 5% CO_2 in air and containing 240 μM DL-histidine. In one batch, the histidine contained only natural-abundance ^{14}N. In the other batch, both of the imidazole nitrogens were ^{15}N-labeled. After 6 days of growth in the light, the cells were harvested and broken with a Bead Beater (Biospec Products, Bartlesville, OK). The thylakoid membranes were washed and an aliquot was taken for determination of the extent of isotopic labeling by mass spectrometry. The remaining thylakoid membranes were extracted with 1% dodecyl maltoside and the extract was subjected to anion-exchange column chromatography on DEAE-Toyopearl 650s (Toso Haas, Philadelphia) (X.-S.T. and B.A.D., unpublished work). The purified PSII core complex showed very high oxygen-evolving activ-

The publication costs of this article were defrayed in part by page charge payment. This article must therefore be hereby marked "*advertisement*" in accordance with 18 U.S.C. §1734 solely to indicate this fact.

Abbreviations: ESEEM, electron spin-echo envelope modulation; OEC, oxygen-evolving complex; PSII, photosystem II; PTC, phenylthiocarbamoyl; PTH, phenylthiohydantoin.

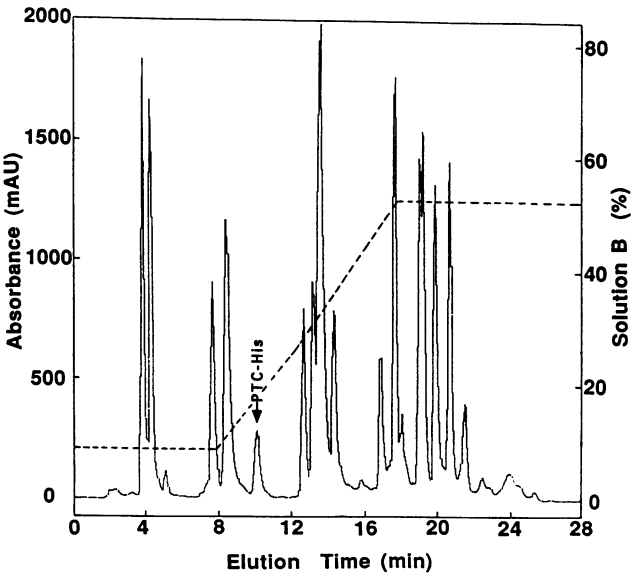

FIG. 1. HPLC elution profile of the mixture of PTC-amino acids obtained by hydrolysis of the thylakoid membranes of *Synechocystis* PCC 6803 and subsequent phenylisothiocyanate derivatization. The point at which standard PTC-histidine is eluted is indicated by the arrow. The dashed line shows the percentage of solution B (see *Materials and Methods*) in the elutant. The absorbance is shown in milliunits at 247 nm.

ity (2400 μmol of O_2 per mg of chlorophyll per hr) under saturating light in the presence of 1 mM 2,5-dichlorobenzoquinone. The PSII complex was first concentrated in an Amicon 8400 ultrafiltration cell fitted with a YM100 membrane and then precipitated with polyethylene glycol 8000. The sample was resuspended in 50 mM Mes/NaOH (pH 6.0) buffer containing 25% (wt/vol) glycerol, 20 mM $CaCl_2$, 5 mM $MgCl_2$, 0.03% dodecyl maltoside, and 0.05 mM ferricyanide. The concentration of the PSII core complexes was adjusted to 3–4 mg of chlorophyll per ml before loading in the dark into an EPR tube.

Derivatization and Mass Analysis of Histidine. The sample of thylakoid membrane set aside for isotopic analysis was completely hydrolyzed in 6 M HCl at 100–110°C for 24 hr. The phenylthiocarbamoyl (PTC) amino acid derivatives were made according to Bidlingmeyer *et al.* (17) from the hydrolysis products by use of phenylisothiocyanate. The PTC-histidine derivative was purified from the other derivatized amino acids by HPLC (Hewlett Packard model 1090M, Waldbronn, Germany) using an ODS Zorbax column (4.6 mm × 150 mm, Rockland Technologies, Newport, DE) according to ref. 18 with the modifications indicated below. The PTC-amino acid mixture, dissolved in 50 μl of 5 mM phosphoric acid/0.95 M acetonitrile, pH 7.4, was injected onto the column, which was preequilibrated with 91% solvent A (0.53 M ammonium acetate, pH 6.5) and 9% solvent B (11.5 M acetonitrile in water), and eluted with a set of linear gradients from 9% to 55% solvent B (Fig. 1). The column was run at 40°C at a flow rate of 0.75 ml/min. Sodium acetate of the original procedure was replaced by ammonium acetate because the latter can be completely removed from the sample by sublimation prior to mass spectral analysis. The separation of the PTC-amino acid derivatives by HPLC is very nearly as good with ammonium acetate as with sodium acetate despite small changes in mobility (Fig. 1). The PTC-histidine peak was identified by determining the mobility of standard PTC-histidine (downward arrow, Fig. 1), and the appropriate fraction was collected. The PTC-histidine was then concentrated to dryness overnight in a Speed Vac (Savant) and the resulting histidine derivative, now largely converted to the phenylthiohydantoin (PTH) amino acid, was

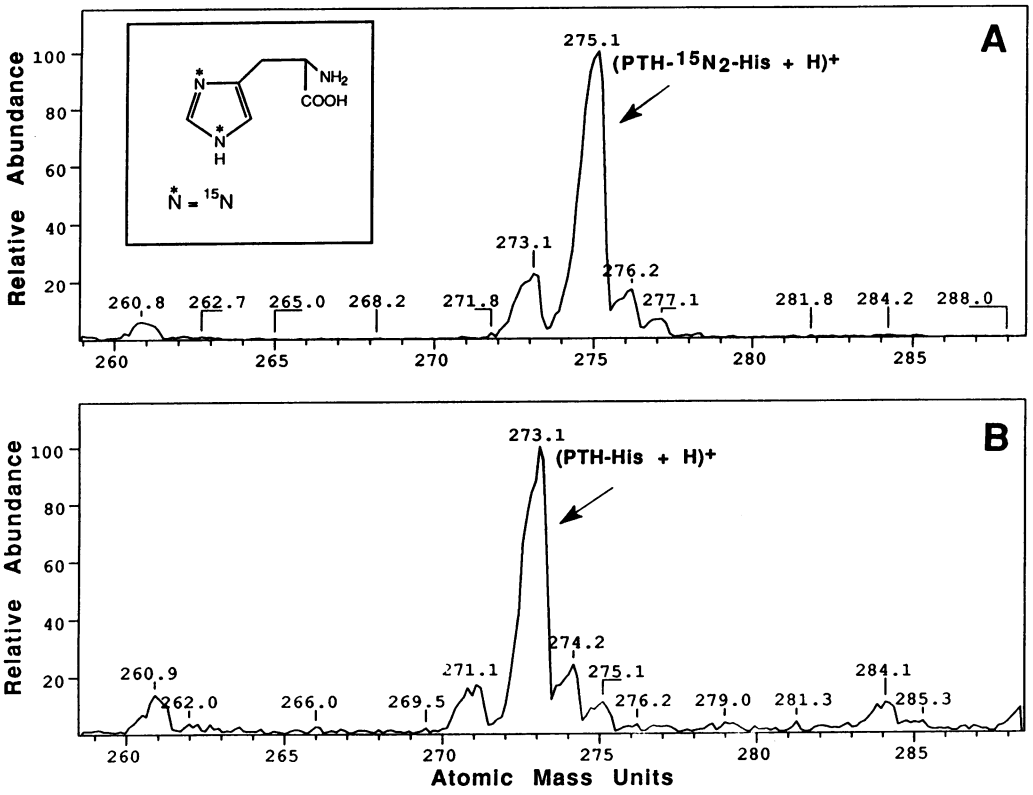

FIG. 2. Mass spectra of PTH-derivatized histidine obtained from histidine-tolerant *Synechocystis* PCC 6803 cells grown with $^{15}N_2$-labeled DL-histidine (*A*) and the ^{14}N analogue (*B*). Spectra were obtained by scanning the mass range 100–800 mass units every 4 sec and averaging 45 scans. (*Inset*) Structural formula of the $^{15}N_2$-labeled histidine.

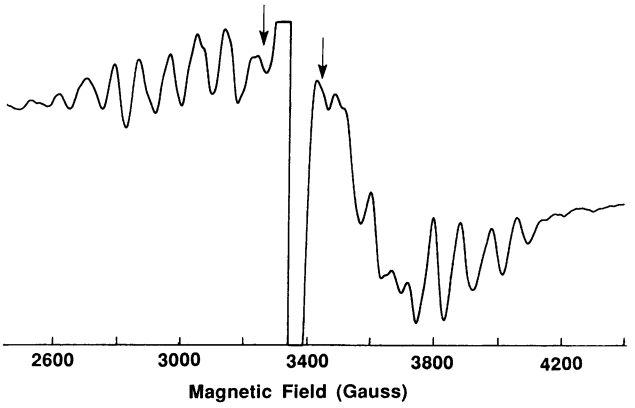

FIG. 3. Light-minus-dark difference continuous-wave EPR spectrum of the S_2 multiline signal in PSII core complex purified from the histidine-tolerant *Synechocystis* PCC 6803 strain grown with [^{14}N]-histidine. The S_2 state of the OEC was light-induced as described in *Materials and Methods*. Instrument conditions: microwave power, 32 mW; time constant, 300 ms; number of scans, 4; field modulation, 20-G amplitude at 100-kHz frequency. Arrows indicate the magnetic fields used in the ESEEM experiments.

resuspended in 60% acetonitrile and subjected to mass analysis. Mass spectra were recorded with a Finnigan–Mat TSQ-700 (San Jose, CA) triple-quadrupole mass spectrometer equipped with an electrospray ion source (Analytica, Branford, CT).

Continuous-Wave and Pulsed EPR Measurements. Low-temperature (10 K) continuous-wave EPR spectra were recorded at X-band with a Bruker ER200D spectrometer equipped with an upgraded computer software system (ESP-300 model) and an Oxford ESR-910 helium flow cryostat. The PSII core complex was dark-adapted in the EPR tube for 30 min on ice. The sample was illuminated in a dry ice/ethanol bath (198 K) for 20 min with saturating white light. ESEEM spectra were recorded with a laboratory-built pulsed EPR spectrometer (19). Light-minus-dark difference spectra, isolating ESEEM contributions from the light-induced $g = 2$ multiline signal, were obtained by subtracting the ESEEM spectra of dark-adapted PSII particles from the spectra obtained after 30 min of illumination at 198 K.

RESULTS

Fig. 2 shows the mass spectra of PTH histidine obtained from the thylakoid membranes of the histidine-tolerant *Synechocystis* PCC 6803 strain, grown in the presence of either 240 μM DL-[$^{15}N_2$]histidine (Fig. 2*A*) or the ^{14}N analogue (Fig. 2*B*). We find a mass peak for PTH histidine only, and none for the PTC derivative. In a control experiment, standard histidine was treated according to the same procedure, and only PTH histidine was found (date not shown). These results

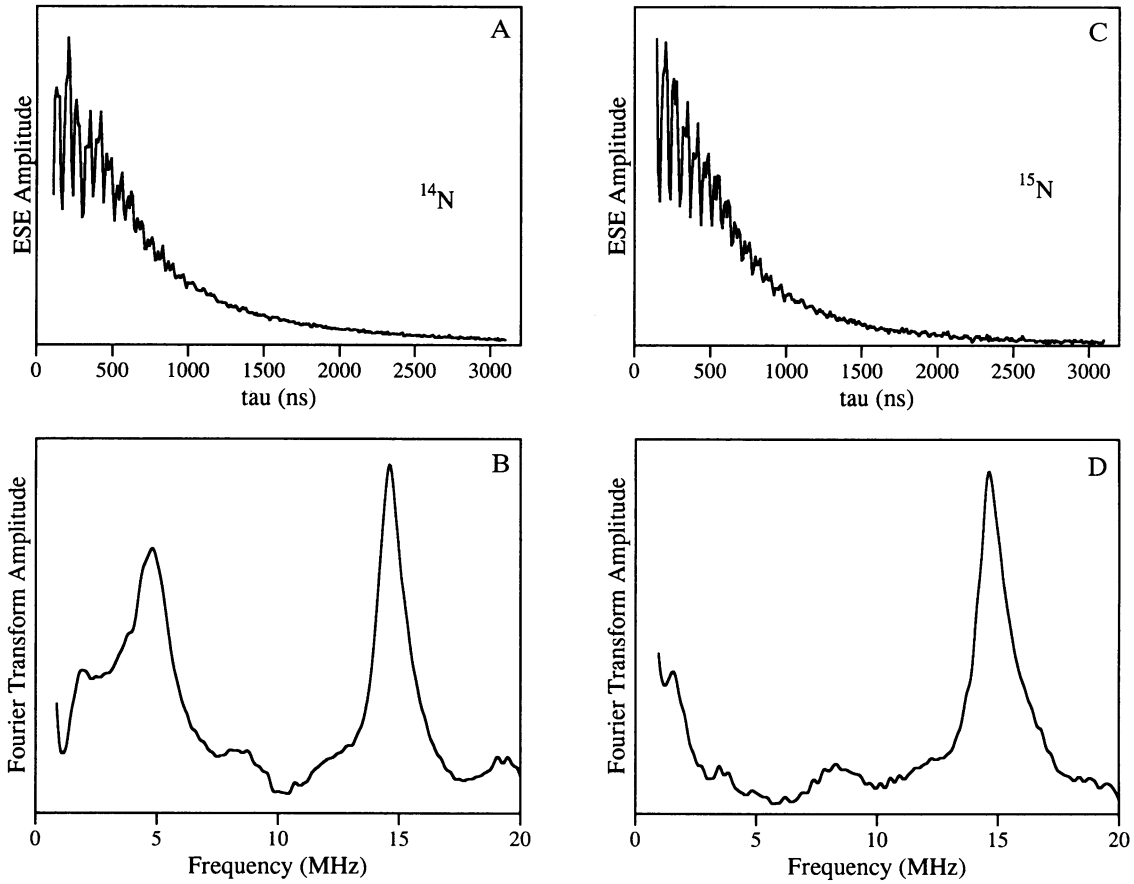

FIG. 4. (*Left*) Two-pulse time-domain ESEEM (*A*) and Fourier transform (*B*) of the $g = 2$ S_2 manganese multiline signal arising from the PSII core complex of *Synechocystis* grown with natural-abundance ^{14}N. (*Right*) Two-pulse time-domain ESEEM (*C*) and Fourier transform (*D*) of the $g = 2$ manganese multiline signal arising from the PSII core complex of *Synechocystis* grown on histidine labeled with ^{15}N at the two imidazole-ring nitrogen positions. The time-domain ESEEM spectra were obtained by subtracting the dark-adapted S_1-state ESEEM spectra from the spectra obtained following 30 min of illumination at 198 K. The spectra were obtained at a magnetic field of 3420 G, a microwave frequency of 9.3607 GHz, a temperature of 4.2 K, and a repetition time between pulse sequences of 2 ms. Microwave pulses were of 12 ns duration with 50-W peak power. The interval τ between pulses in the two-pulse sequence was increased from 110 ns to 3100 ns in 10-ns τ increments. ESE, electron spin-echo.

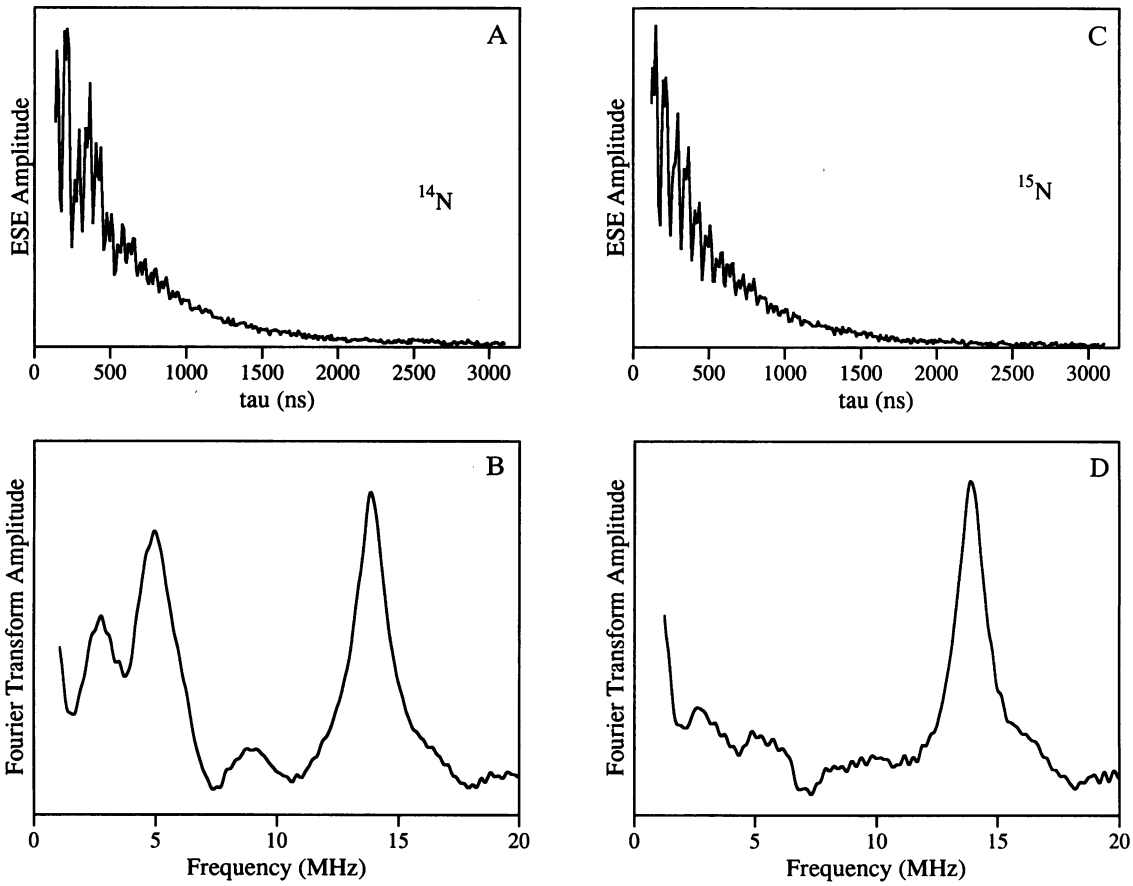

FIG. 5. Identical to Fig. 4 except for the magnetic field value of 3260 G.

indicate that the PTC-histidine was converted to the PTH derivative upon drying overnight in the Speed Vac. When cells were grown in the presence of 240 μM DL-[$^{15}N_2$]-histidine, 85% of the histidine molecules incorporated into the thylakoid proteins were labeled with ^{15}N at both nitrogens of the imidazole ring. The remaining histidines, arising from low-level endogenous histidine biosynthesis, had ^{14}N at both nitrogens (Fig. 2). There was no singly or triply labeled amino acid, indicating that ^{15}N was not appearing at any appreciable level in the endogenous cellular nitrogen pool. A similar labeling percentage was found when the above described analysis was performed directly on the PSII core complexes used in the ESEEM experiments (data not shown).

A normal $g = 2$ multiline EPR signal (Fig. 3), arising from the S_2 redox state of the manganese cluster (2), was observed in the PSII core complex purified from the histidine-tolerant mutant cells grown in the presence of [^{14}N]histidine. An identical EPR spectrum was observed in the [^{15}N]histidine-labeled PSII complex (data not shown) and showed no effect of isotopic substitution. The field-swept pulsed EPR spectra are very similar to previously published electron spin-echo field sweeps of the $g = 2$ multiline signal (6, 12, 20) (data not shown).

Fig. 4*A* and *B* display the time- and frequency-domain two-pulse ESEEM patterns recorded at the field value of 3420 G for the cyanobacteria grown on natural-abundance ^{14}N. The ^{14}N peak centered near 5 MHz is similar to that previously reported (6, 7, 12). The other feature at 15 MHz arises from weakly coupled protons resonating at or near the proton Larmor frequency. Fig. 4*C* and *D* show the ESEEM patterns obtained for the cyanobacteria with ^{15}N-labeled histidine. The ^{14}N ESEEM peaks are no longer present. Parallel results recorded at a field value of 3260 G show the same effect (Fig. 5). These results clearly demonstrate that the imidazole side chain of histidine is the source of the nitrogen modulation. Recent multifrequency ESEEM experiments measuring the magnetic field dependence of the ^{14}N ESEEM in spinach preparations have demonstrated that the peak arises from a "single-quantum" ^{14}N spin transition (B. E. Sturgeon, M.L.G., J. A. Ball, and R.D.B., unpublished work). ^{14}N single-quantum transitions occur in this frequency range when both the isotropic and anisotropic components of the ^{14}N hyperfine interaction are large (11), and such an interaction has been observed to result in no detectable ESEEM upon ^{15}N substitution (11). The magnitude of the hyperfine interaction is actually greater than observed for some classes of nitrogen ligands in Mn(III)-Mn(IV) model systems (refs. 12 and 13; B. E. Sturgeon, W. A. Armstrong, M. P. Klein, and R.D.B., unpublished work), and we consider this large hyperfine interaction to be very strong evidence that the imidazole nitrogen is directly coordinated to manganese of the catalytic cluster. Because of the large degree of anisotropy in the hyperfine interaction, it is difficult to determine if the measured ESEEM pattern results from more than one ^{14}N nucleus. Since the experiment was performed with doubly labeled histidine, the results do not indicate which of the two imidazole nitrogens is ligated to manganese. In fact, we cannot rule out the possibility that both imidazole nitrogens are ligands, i.e., that the histidine side chain forms an imidazolate bridge between two manganese ions.

DISCUSSION

The presence of this histidine ligand at the catalytic site is probably crucial to the catalytic cycle. The presence of histidine as a coordinating ligand to the manganese cluster is consistent with the results of extensive site-directed muta-

genesis of the *psbA* gene, which encodes the D1 polypeptide of the PSII reaction center. The OEC is bound on the luminal side of the thylakoid membrane, and the reaction center polypeptides D1 and D2 are the most likely candidates for coordination of the manganese cluster (see ref. 21 for a review). Nixon and Diner and colleagues (refs. 22 and 23; unpublished work) and Debus (21) have found that amino acid replacement of histidine-190 or histidine-332 on the luminal side of D1 results in the loss of oxygen-evolving activity. As there are no other essential histidine residues on the luminal sides of polypeptide D1 (refs. 21–23; and P. J. Nixon and B.A.D., unpublished results) or D2 (24), it is likely that one or possibly both of these histidines are coordinating ligands.

In addition to its structural role as a ligand to the manganese cluster, it is possible that a histidine ligand could serve a role in proton conduction from oxidized water to the lumenal phase inside the photosynthetic thylakoid membrane. It is known that protons are released, coupled to the oxidation of the OEC (25). While the net release ultimately arises from water, those protons released upon individual oxidation steps are contributed in part by the deprotonation of ligands or of residues in the vicinity of the manganese cluster. In the imidazole and histidine coordination-chemistry literature there are numerous examples where metal binding to the N_3 "pyridine" nitrogen of imidazole greatly increases the acidity of the remote N_1 "pyrrole" nitrogen over that of free imidazole ($pK_a > 14$) (26, 27). The specific pK_a value depends on both the metal and the other ligands to the metal, but reduction of pK_a values by 4 logarithmic units is not atypical (26, 27). In addition, the presence of a second metal ion can assist the deprotonation via a proton–metal substitution reaction resulting in the formation of an imidazolate bridge. In the OEC, the pK_a of the remote nitrogen of a histidine imidazole group ligated to manganese would be decreased relative to that of an unbound histidine imidazole. The remote nitrogen could undergo a further decrease in pK_a and release its proton in response to manganese oxidation at some S-state transition. Binding of a proton released by water oxidation could then occur at the final, $S_4 \rightarrow S_0$ step of the cycle as the nitrogen basicity increases with the re-reduction of manganese. It is also possible that the nitrogen deprotonation could be assisted by binding to a second high-valence manganese, with the formation of an imidazolate bridge within the manganese cluster. Again, upon reduction of manganese during the $S_4 \rightarrow S_0$ transition, this imidazolate bridge could be broken, with the concomitant acceptance of a proton released from water. This would provide a proton-transfer mechanism similar to that proposed for the role of the imidazolate bridge in Cu–Zn superoxide dismutase (28).

A histidine has been reported to be oxidized upon illumination of Ca^{2+}-depleted PSII-enriched membrane fragments (29). Whether there is any relation between the histidine ligand described here and this oxidized residue is unclear.

We thank Bradley E. Sturgeon for technical assistance with the pulsed EPR spectroscopy. B.A.D. gratefully acknowledges support from a National Research Initiative Competitive Grants Program grant from the U.S. Department of Agriculture. R.D.B. gratefully acknowledges support from the Camille and Henry Dreyfus Foundation, a grant from the National Institutes of Health, and a National Research Initiative Competitive Grants Program grant from the U.S. Department of Agriculture. ^{15}N-labeled histidine was provided by the National Institutes of Health National Stable Isotope Resource of the Los Alamos National Laboratory.

1. Joliot, P. & Kok, B. (1975) in *Bioenergetics of Photosynthesis*, ed. Govindjee (Academic, New York), pp. 387–412.
2. Dismukes, G. C. & Siderer, Y. (1981) *Proc. Natl. Acad. Sci. USA* **78,** 274–278.
3. Casey, J. L. & Sauer, K. (1984) *Biochim. Biophys. Acta* **767,** 21–28.
4. Zimmermann, J.-L. & Rutherford, A. W. (1984) *Biochim. Biophys. Acta* **767,** 160–167.
5. Sauer, K., Yachandra, V. K., Britt, R. D. & Klein, M. P. (1992) in *Manganese Redox Enzymes*, ed. Pecoraro, V. L. (VCH, New York), pp. 141–175.
6. Britt, R. D., Zimmermann, J.-L., Sauer, K. & Klein, M. P. (1989) *J. Am. Chem. Soc.* **111,** 3522–3532.
7. DeRose, V. J., Yachandra, V. K., McDermott, A. E., Britt, R. D., Sauer, K. & Klein, M. P. (1991) *Biochemistry* **30,** 1335–1341.
8. Mims, W. B. (1972) *Phys. Rev. B* **5,** 2409–2419.
9. Flanagan, H. L. & Singel, D. J. (1987) *J. Chem. Phys.* **87,** 5606–5616.
10. Lai, A., Flanagan, H. L. & Singel, D. J. (1988) *J. Chem. Phys.* **89,** 7161–7166.
11. McCracken, J., Peisach, J., Cote, C. E., McGuirl, M. A. & Dooley, D. M. (1992) *J. Am. Chem. Soc.* **114,** 3715–3720.
12. Britt, R. D. (1988) Thesis (University of California, Berkeley).
13. Britt, R. D. & Klein, M. P. (1992) in *Pulsed Magnetic Resonance: NMR, ESR, and Optics*, ed. Bagguley, D. M. S. (Clarendon, Oxford), pp. 390–410.
14. Tang, X.-S., Sivaraja, M. & Dismukes, G. C. (1993) *J. Am. Chem. Soc.* **115,** 2382–2389.
15. Labarre, J., Thuriaux, P. & Chauvat, F. (1987) *J. Bacteriol.* **169,** 4668–4673.
16. Rippka, R., Deruelles, J., Waterbury, J. B., Herdman, M. & Stanier, R. Y. (1979) *J. Gen. Microbiol.* **111,** 1–61.
17. Bidlingmeyer, B. A., Cohen, S. A. & Tarvin, T. A. (1984) *J. Chromatogr.* **336,** 93–97.
18. Gimenez-Gallego, G. & Thomas, K. A. (1987) *J. Chromatogr.* **409,** 299–304.
19. Sturgeon, B. E. & Britt, R. D. (1992) *Rev. Sci. Instrum.* **63,** 2187–2192.
20. Zimmermann, J.-L., Boussac, A. & Rutherford, A. W. (1993) *Biochemistry* **32,** 4831–4841.
21. Debus, R. J. (1992) *Biochim. Biophys. Acta* **1102,** 269–352.
22. Diner, B. A., Nixon, P. J. & Farchaus, J. W. (1991) *Curr. Opin. Struct. Biol.* **1,** 546–554.
23. Nixon, P. J., Chisholm, D. A. & Diner, B. A. (1992) in *Plant Protein Engineering*, eds. Shewry, P. & Gutteridge, S. (Cambridge Univ. Press, Cambridge, U.K.), pp. 93–141.
24. Pakrasi, J. B. & Vermaas, W. F. J. (1992) in *The Photosystems: Structure, Function, and Molecular Biology*, ed. Barber, J. (Elsevier, Amsterdam), pp. 231–257.
25. Rappaport, F. & Lavergne, J. (1991) *Biochemistry* **30,** 10004–10012.
26. Sundberg, R. J. & Martin, R. B. (1974) *Chem. Rev.* **74,** 471–517.
27. Kiss, T. (1990) in *Biocoordination Chemistry: Coordination Equilibria in Biologically Active Systems*, ed. Burger, K. (Horwood, New York), pp. 56–134.
28. Tainer, J. A., Getzoff, E. D., Richardson, J. S. & Richardson, D. C. (1983) *Nature (London)* **306,** 284–287.
29. Boussac, A., Zimmermann, J.-L., Rutherford, A. W. & Lavergne, J. (1990) *Nature (London)* **347,** 303–306.